PROCEEDINGS OF SPIE

SPIEDigitalLibrary.org/conference-proceedings-of-spie

The Subaru coronagraphic extreme AO (SCExAO) system: visible imaging mode

Garrel, Vincent, Guyon, Olivier, Baudoz, Pierre, Martinache, Frantz, Vogt, Frederic, et al.

Vincent Garrel, Olivier Guyon, Pierre Baudoz, Frantz Martinache, Frederic Vogt, Yoshikawa Takashi, Yokochi Kaito, Faustine Cantalloube, "The Subaru coronagraphic extreme AO (SCExAO) system: visible imaging mode," Proc. SPIE 7736, Adaptive Optics Systems II, 77365V (28 July 2010); doi: 10.1117/12.857874

SPIE.

Event: SPIE Astronomical Telescopes + Instrumentation, 2010, San Diego, California, United States

The Subaru coronagraphic extreme AO (SCExAO) system: visible imaging mode

Vincent Garrel [a,b], Olivier Guyon[a], Pierre Baudoz[b], Frantz Martinache[a], Frederic Vogt [a], Yoshikawa Takashi [a], Yokochi Kaito[a] and Faustine Cantalloube[a]

[a] Subaru Telescope, 650 N. A'Ohoku, Hilo, USA;
[b] LESIA, 4 places Jules Janssen, Meudon, France

ABSTRACT

The Subaru Coronagraphic Extreme Adaptive Optics (SCExAO) system is an instrument designed to be inserted between the Subaru AO188 system and the infrared HiCIAO camera in order to greatly improve the contrast in the very close (less than 0.5") neighbourhood of stars. Next to the infrared coronagraphic path, a visible scientific path, based on a EMCCD camera, has been implemented. Benefiting from both Adaptive Optics (AO) correction and new data processing techniques, it is a powerful tool for high angular resolution imaging and opens numerous new science opportunities. We propose here a new image processing algorithm, based on the selection of the best signal for each spatial frequency. A factor 2 to 3 in Strehl ratio is obtained compared to the AO long exposure time depending on the image processing algorithm used and the seeing conditions. The system is able to deliver diffraction limited images at 650 nm (17 mas FWHM).We also demonstrate that this approach offers significantly better results than the classical select, shift and add approach (lucky imaging).

Keywords: instrumentation: high angular resolution instrumentation: adaptive optics methods: data analysis techniques: high angular resolution techniques: image processing

1. INTRODUCTION

The angular resolution of large ground based telescope is not limited by the theoritical diffraction limit but by the wavefront distortion induced by the atmospheric turbulence. Over the years, great efforts have been devoted to partially or completely recover this otherwise lost spatial information. The most successful technique is probably the adaptive optics systems, performing a real-time phase wavefront correction in parallel of the instrument acquisition. AO systems achieve routinely high correction of wavefront aberrations in the near infrared producing high Strehl ratio images. However due to the stronger and faster phase distortion, AO systems are still technologically struggling to perform a valuable correction in the visible band. Another set of techniques, called under the general name of speckle imaging, is based on the atmospheric coherence time, typically a few milliseconds to tens of milliseconds. An image recorded faster than this coherence time records an object distorted by a frozen wavefront still holding high spatial frequencies, up to the diffraction limit of the telescope. These techniques are numerous, we can cite the speckle interferometry,[1] the speckle masking technique[2] or the Lucky imaging[3] among many others... The Lucky imaging technique recently gained a new interest with the avaibility of EMCCD camera,[4] featuring virtually no readout noise and a photocounting ability, allowing instruments to shorten their exposure time with a minimal loss on their SNR even for low light intensity. More recently these technique have been combined with an AO system, showing promising results for bigger telescopes.[5]

In section 2 we will describe our instrument setup and its goal. Then we will explain a new algorithm for the visible imaging mode in section 3. In the following section 4 we detail the conditions of our simulation and present our first results. Finally, in section 5 we will conclude.

Further author information: (Send correspondence to Vincent Garrel)
Vincent Garrel: E-mail: vgarrel@subaru.naoj.org

Adaptive Optics Systems II, edited by Brent L. Ellerbroek, Michael Hart, Norbert Hubin, Peter L. Wizinowich,
Proc. of SPIE Vol. 7736, 77365V · © 2010 SPIE · CCC code: 0277-786X/10/$18 · doi: 10.1117/12.857874

2. SCEXAO

SCExAO is a new high resolution instrument designed to offer coronagraphic extreme AO capability (ExAO) to the recently comissionned HiCIAO imager instrument.[6] The system will take over the wavefront corrected beam after the current and independent AO188 and will offer a second stage of AO correction based on a Boston Micromachine 1K MEMS. The wavefront control architecture is optimized for high contrast imaging, and includes a dedicated low order wavefront sensor using light reflected by the coronagraph focal plane mask. Custom optics able to remove spiders from the telescope pupil, and PIAA lenses performing lossless beam apodization will give SCExAO the ability to efficiently deliver high contrast as close as 1 λ/D. The becnh design is meant to bring versatility to the experiment so new interesting coronagraphic features can be easily implemented and tested. HiCIAO is mainly working in H band and the AO188 offers a mode where it uses visible light down to only λ=630nm. We decide to take advantage of the available red band, from 630 to 800nm to open a new scientific path. The new instrument is a red band imager based on a 512 by 512 pixels EMCCD Andor Camera, taking series of short exposures frames. This instrument will be able to deliver red band images with a diffraction limited core, the first instrument to our knowledge to do so for a 8 meter class telescope at this band. In combination with HiCIAO, this scientific imager will open a new window for stellar environment, active galactic nuclei, or small planetary objects study. SCExAO is currently under integration and testing, and is scheduled for first light on the Subaru Telescope in early 2011.

3. ALGORITHM

3.1 Introduction

This algorithm is designed to provide a high resolution image from a serie of short exposures frames. For these kind of frames, PSFs doesn't have the typical gaussian aspect but look much more ruggerized, a pattern known as speckles. The speckles arises because of interferences from the wavefront aberrations in the pupil due to atmospheric turbulence. Since these aberrations are realizations of a random process, it has been shown[3] that sometimes the wavefront aberrations are small all over the pupil, producing a PSF close to the theoritical one of the telescope. Adaptive optics system by correcting the wavefront distortion, increases the probability of such realizations.[7] The probability still remains low mainly because actual AO systems lacks of actuators and have too slow temporal response.

3.2 Image Formation Model

To understand our algorithm, we can describe images as the convolution of an object by the short exposure PSF, ie the response of an imaging system composed by the turbulent atmosphere and the telescope system at a given time. As each images of the serie is under the atmospheric coherence time, each PSF is different. We note * the convolution operator.

$$Image_n(x,y) = Object(x,y) * PSF_n(x,y) \tag{1}$$

However we can also describe the PSF as its fourier transform, the optical transfer function (OTF). The OTF of the system is simply the multiplication the atmosphere OTF by the telescope OTF. OTFs are spatial frequency filters, with a different contributions for each frequency. $\mathcal{F}$ design the fourier transform.

$$\mathcal{F}(Image_n(x,y)) = \mathcal{F}(Object(x,y)).OTF_n(f_x,f_y) \tag{2}$$

The Optical Transfer Function can be described as a Telescope Transfer Function and an Atmosphere transfer function. We can safely assume the telescope transfer function is static during the acquisition.

$$OTF_n(f_x,f_y) = OTF_{telescope}(f_x,f_y).OTF_{n/atmopshere}(f_x,f_y) \tag{3}$$

We can also decompose the complex atmospheric OTF as its amplitude, the Modulation Transfer Function and its phase, the Phase Transfer Function.

$$OTF_n(f_x, f_y) = |OTF_n(f_x, f_y)|.\exp(-2i\pi\lambda(f_x, f_y)) = MTF_n(f_x, f_y).PTF_n(f_x, f_y) \tag{4}$$

Since the atmospheric turbulence is mainly a phasing contribution, it can be shown easily that the telescope diffraction limited perfect case is the maximum amplitude response possible for each frequency.

$$MTF(f_x, f_y)_{telescope} > MTF(f_x, f_y)_{telescope}.MTF_n(f_x, f_y)_{atmosphere} \tag{5}$$

$$MTF(f_x, f_y)_{telescope} > MTF_n(f_x, f_y)_{system} \tag{6}$$

3.3 Algorithm in the noiseless case

The last equation shows us than if we select for each spatial frequency the highest amplitudes, the recovered information is closer from the perfect case where the telescope alone is considered. These highest amplitudes can be picked in any place in the serie of images. If the amplitude is close to the perfect case, it also mean that the unphasing brought by the atmosphere turbulence is small. So the algorithm will select the phase associated to the chosen highest amplitude. Once the selection done, we use an inverse transform transform before stacking images. Figure 1 described how our algorithm is applied to the data.

3.4 Comparison with Lucky Imaging

Our algorithm shares some features with the classical Lucky Imaging technique. They both recenter images between them, which correspond to the correction of tip-tilt. They both select a part of the information to improve the image resolution. Their difference stands in the way algorithms select their information.

As a reminder, the Lucky Imaging uses a quality criterion that assess if a particular image in a serie is better than most. Several criterions have been proposed but the Sthrel ratio is the most used for its simplicity[84] and its direct relation to wavefront aberrations (when the Marechal criterion is met).

Where classical Lucky Imaging uses quality criterions for the PSF and preserves the image unity, our algorithm use a quality criterion for each spatial frequency and doesn't preserve the image unity.

3.5 Algorithm in a photon-noise case

We will take now into account photon noise, a strong factor in the short exposure low light case. Photon noise in the fourier plane have been shown to add a white noise,[9] its level only dependent of the image photometry. We describe it as an additional noise in the following equation:

$$\mathcal{F}(I_n(x, y)) = \mathcal{F}(Object(x, y)).OTF_n(f_x, f_y) + B_n \tag{7}$$

Our algorithm is naturally very sensitive to photon noise since it will tend to select the upper realizations of the poissonian distribution described by the photon noise. One way to mitigate this problem rely on the fact the MTF of atmospheric distortion is locally very spatially correlated whereas the photon noise, a white noise in the fourier plane, is totally spatially uncorrelated. We propose to proceed to the selection after the MTF have been artificially blurred by a small gaussian kernel. This way, the photon noise is quickly averaged but the selection of good MTF signal is much less affected. However the signal is still picked in the noised unblurred case to preserve the resolution. Figure 2 describes our algorithm for the noisy case.

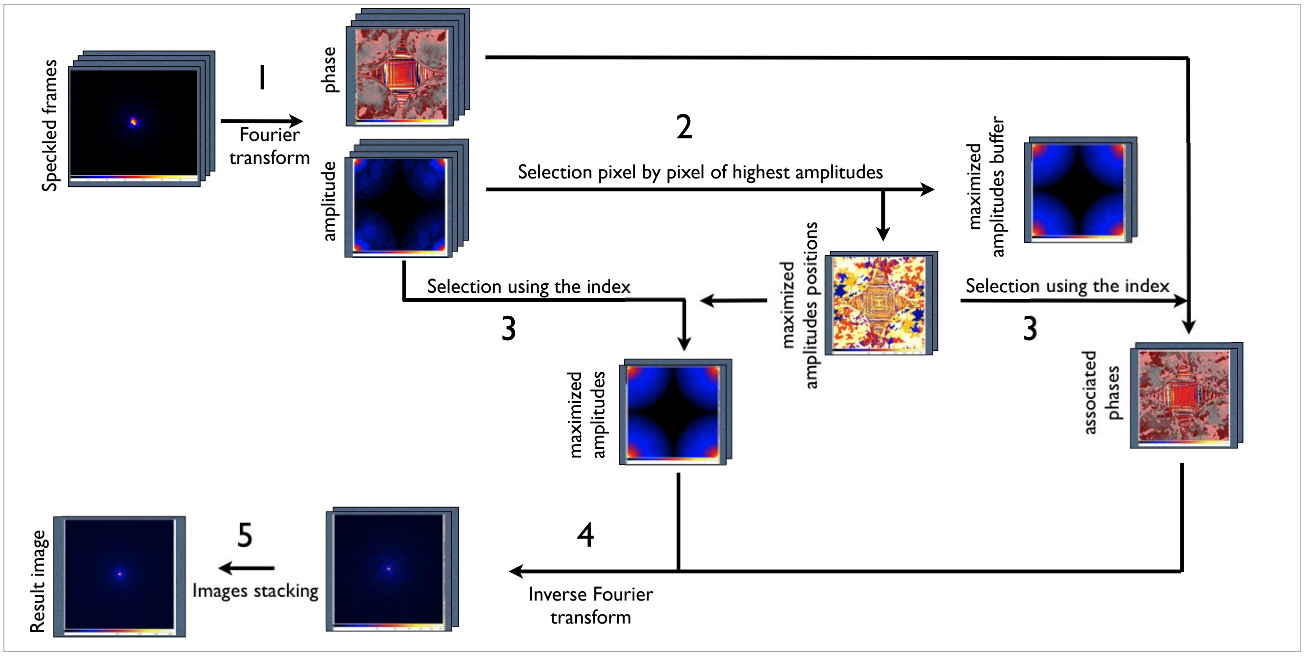

Figure 1. Algorithm for the case when no photon noise is taken into account. Each step is numbered to describe the succession of operations. Horizontal label design operations themselves. Vertical label design results of each operation. To ease the figure, images in the serie have already been recentered between them. The selection rate is user dependent.

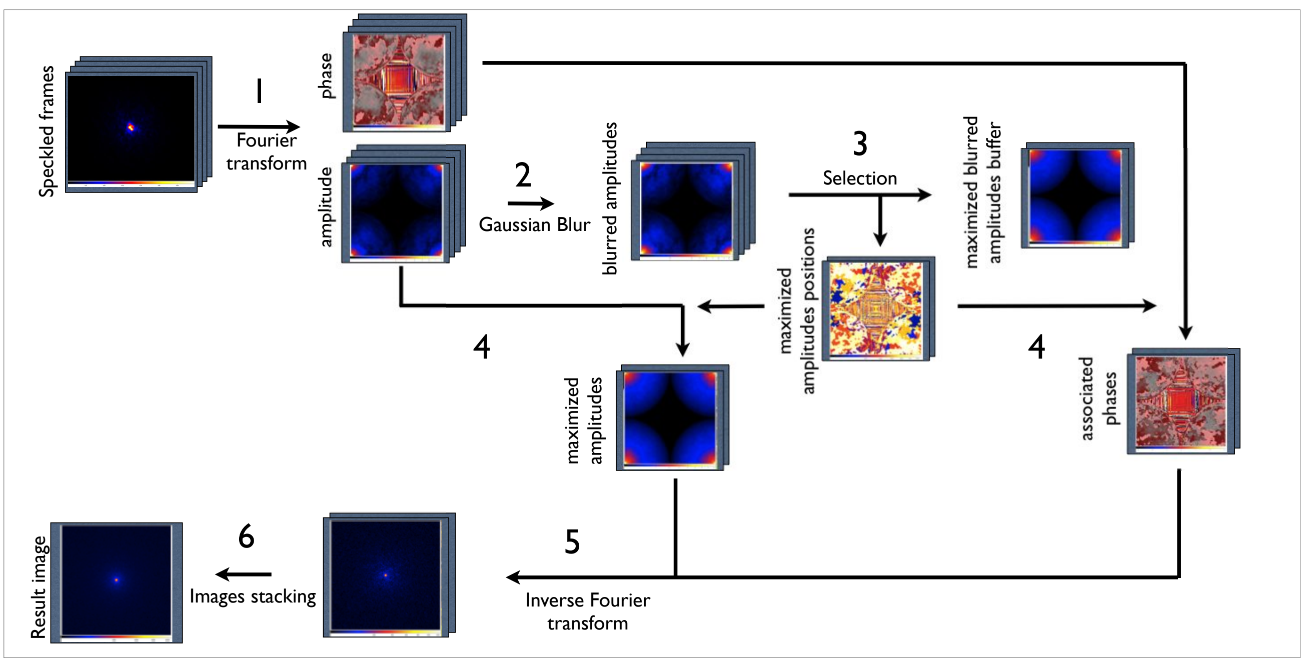

Figure 2. Algorithm for the case when photon noise is taken into account. Each step is numbered to describe the succession of operations.Horizontal label design operations themselves. Vertical label design results of each operation. Images inside the serie have already been recentered between them. The selection rate is user dependent. The difference with the precendent algorithm lies in the gaussian blur operation.

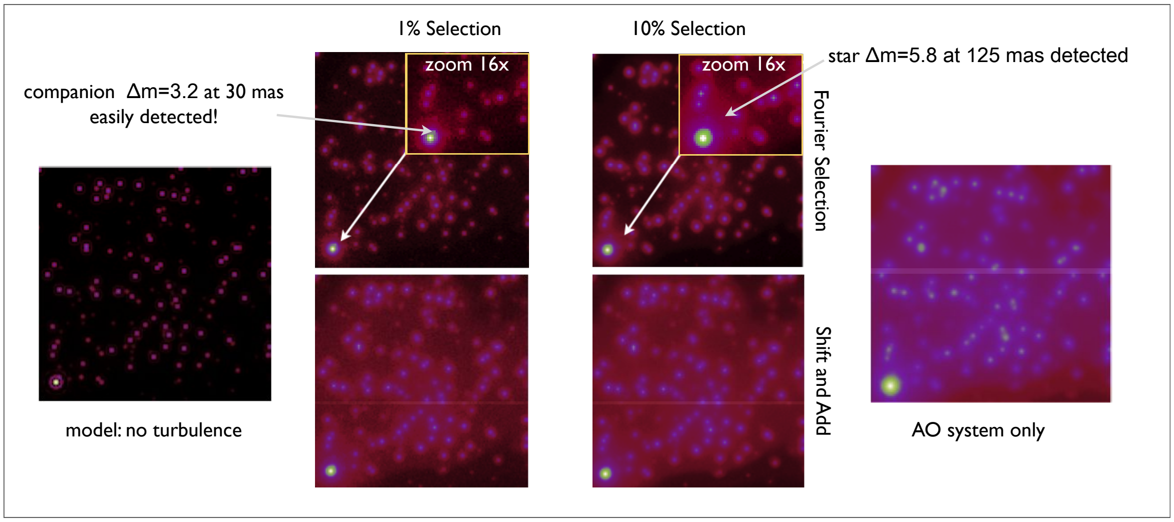

Figure 3. A crowded star field. The guide star is at the bottom on the left. On the left image: the perfect case of the simulated star field without any turbulence. On the right image: the long exposure AO case without any data processing. On the top: images from our algorithm for a 1% and 10% selection process. On the bottom: images from the Lucky Imaging.

4. SIMULATION AND RESULTS

Realistic closed loop simulations of Subaru's AO188 system were used to provide inputs for the visible imager simulation. The simulation tool includes major sources of error in the AO system, including photon noise in the wavefront sensor, fitting errors due to the DM actuators and temporal lag. The simulation tool is closely reproducing key hardware in the AO system, including the wavefront sensor lenslet geometry, bimorph geometry, and wavefront sensor throughput. The performance obtained by the simulation tool has been verified to be consistent with actual on-sky performance.

From the set of H band phase screens issued by the AO188 simulation, we modeled a serie of abberatted psf set at λ=650nm. Then we convolved them by any science object we are interested to model. Finally we binned theses images to adjust the frequency of temporal sampling, from the 2kHz AO sampling time to the tens of Hz for the camera sampling. The particular serie we are using in these paper is based on a field of 1 main star of 11th magnitude, used as a guide star by the AO system surrounded by 10 to 1000 time weaker stars. We simulate a narrow band of 10 nm around the central wavelength. The seeing was chosen to be 0.6, a slightly better than average value for Mauna Kea. The serie itself is composed of 8200 images, sampled at 35Hz, representing almost 4 minutes of exposure time. The images have been fourier zoomed by a factor 4 to determine their brightest pixel, we use this brightest pixel as center which is described as the most efficient procedure.[10] Images have been recentered by subpixel translation using the fourier translation technique.

We compare in Figure 3, images from our algorithm with images taken by a classical Lucky Imaging procedure on the same serie of images.Images have been recentered before any selection by our algorithm or the Lucky Imaging.We applied a 1% and a 10% selection process. A Strehl ratio evaluation is not possible in this crowded field however as the object is known, it is easy to assess the magnitude difference and the angular separation of stars and compare the image quality in term of detection with the classical Lucky Imaging. Our algorithm allows the easy detection of a companion for the guide star at 30 mas of separation with a 3.2 difference in magnitude for the 1% selection process. For the 10% the better quality of the result image is obvious with a halo much dimmer than the one in the lucky imaging. It allows a detection of a faint companion at 125mas with a 5.8 magnitude in difference.

5. DISCUSSION AND CONCLUSION

The gaussian blurring approach is a good first approach to mitigate the photon noise but need some refinement. We will next assess signal to noise ratio taking into account the atmospheric noise and the photon noise. With a better statistical understanding we should improve our selection algorithm. We will assess more quantitavely the image quality in a near future but this new algorithm looks to increase greatly the spatial resolution and contrast of images based on series of short exposure frames compared to the Lucky Imaging technique. This finer algorithm and a larger telescope diameter compared to the current state of art will hopefully bring the finest resolution ever obtained in the visible. We will use this visible imaging mode of SCExAO on-sky with Subaru Telescope next winter.

REFERENCES

1. A. Labeyrie, "Attainment of Diffraction Limited Resolution in Large Telescopes by Fourier Analysing Speckle Patterns in Star Images," *Astronomy and Astrophysics* **6**, pp. 85–+, May 1970.
2. G. P. Weigelt, "Modified astronomical speckle interferometry 'speckle masking'," *Optics Communications* **21**, pp. 55–59, Apr. 1977.
3. D. L. Fried, "Probability of getting a lucky short-exposure image through turbulence," *Journal of the Optical Society of America (1917-1983)* **68**, pp. 1651–1658, Dec. 1978.
4. F. Hormuth, W. Brandner, S. Hippler, and T. Henning, "AstraLux - the Calar Alto 2.2-m telescope Lucky Imaging Camera," *Journal of Physics Conference Series* **131**, pp. 012051–+, Oct. 2008.
5. N. M. Law, C. D. Mackay, R. G. Dekany, M. Ireland, J. P. Lloyd, A. M. Moore, J. G. Robertson, P. Tuthill, and H. C. Woodruff, "Getting Lucky with Adaptive Optics: Fast Adaptive Optics Image Selection in the Visible with a Large Telescope," *Astrophysical Journal* **692**, pp. 924–930, Feb. 2009.
6. K. W. Hodapp, R. Suzuki, M. Tamura, L. Abe, H. Suto, R. Kandori, J. Morino, T. Nishimura, H. Takami, O. Guyon, S. Jacobson, V. Stahlberger, H. Yamada, R. Shelton, J. Hashimoto, A. Tavrov, J. Nishikawa, N. Ukita, H. Izumiura, M. Hayashi, T. Nakajima, T. Yamada, and T. Usuda, "HiCIAO: the Subaru Telescope's new high-contrast coronographic imager for adaptive optics," in *Society of Photo-Optical Instrumentation Engineers (SPIE) Conference Series*, *Presented at the Society of Photo-Optical Instrumentation Engineers (SPIE) Conference* **7014**, Aug. 2008.
7. M. P. Cagigal and V. E. Canales, "Generalized Fried parameter after adaptive optics partial wave-front compensation.," *Journal of the Optical Society of America A* **17**, pp. 903–910, May 2000.
8. J. E. Baldwin, R. N. Tubbs, G. C. Cox, C. D. Mackay, R. W. Wilson, and M. I. Andersen, "Diffraction-limited 800 nm imaging with the 2.56 m Nordic Optical Telescope," *Astronomy and Astrophysics* **368**, pp. L1–L4, Mar. 2001.
9. J. W. Goodman and J. F. Belsher, "Fundamental limitations in linear invariant restoration of atmospherically degraded images," in *Society of Photo-Optical Instrumentation Engineers (SPIE) Conference Series*, J. C. Wyant, ed., *Presented at the Society of Photo-Optical Instrumentation Engineers (SPIE) Conference* **75**, pp. 141–154, 1976.
10. J. C. Christou, "Image quality, tip-tilt correction, and shift-and-add infrared imaging," *Publications of the ASP* **103**, pp. 1040–1048, Sept. 1991.